A Dual-Space Feedforward PID Control of Redundantly Actuated Parallel Manipulators with Real-Time Experiments

Guilherme Sartori Natal, Ahmed Chemori, Micaël Michelin, François Pierrot

A Dual-Space Feedforward PID Control of Redundantly Actuated Parallel Manipulators with Real-Time Experiments

G. Sartori Natal * **A. Chemori** * **M. Michelin** ** **F. Pierrot** *

* *LIRMM, Univ. Montpellier 2 - CNRS, 161 rue Ada, 34392 Montpellier, France (e-mail: sartorinatal@lirmm.fr).*
** *Tecnalia Cap Omega, Rd-Pt B. Franklin, 34960 Montpellier CEDEX 2 - France (e-mail: micael.michelin@tecnalia.com).*

Abstract: This paper deals with dual-space control of R4 redundantly actuated parallel manipulator for very high acceleration applications. This controller consists in a PID in the Cartesian space complied with a feedforward of the desired acceleration in both Cartesian and articular spaces for tracking performance improvements: models show that this "dual-space" control strategy is an efficient way to implement computed torque control. For comparison purposes, experiments were made with a Cartesian PID until 20G. Experimental results show that the proposed control scheme is considerably better than the PID in the Cartesian space, and that a good tracking performance could be achieved even for the very high acceleration of 40G (equivalent to more than 425 pick-and-place cycles per minute).

Keywords: Actuation redundancy, robotics, Parallel manipulators, motion control, PID control, feedforward.

In order to perform very high speed/acceleration tasks, it is well known that parallel manipulators have important advantages in comparison to serial manipulators. One of its main disadvantages, however, is the abundance in singularities in the workspace Kock and Schumacher (1998). If singularities cannot always be eliminated by actuation redundancy, their locii can be modified Park and Kim (1999). Actuation redundancy might also be a way to reach higher accelerations or to improve the homogenity of accelation performance over the workspace (this was the basic conjecture in Corbel et al. (2010), and can also allow for more safety in case of breakdown of individual actuators Yi et al. (2006),Roberts et al. (2008).

Considering these features, the R4 parallel manipulator Corbel et al. (2010) (which can be seen as a redundant Delta robot Clavel (1988)), has three degrees-of-freedom (*dof*) and four actuators. It was designed to have in theory the capability of reaching 100G of acceleration. The number of actuators was chosen such that a good compromise between the gain in acceleration capabilities and the overall cost of the robot could be obtained.

In the literature, several control schemes of parallel manipulators in joint space and in Cartesian space have been proposed. In the joint space, Proportional-Derivative (PD) controllers were implemented in Ghorbel et al. (2000),Wu et al. (2002), PID controllers tuned with elaborated methods (adapted for Parallel Kinematic Machines: PKMs) were proposed in Zhiyong and Huang (2004),Yang et al. (2006), nonlinear PD control was proposed in Ouyang et al. (2002),Su et al. (2004) and artificial-intelligence based control in Begon et al. (1995),Chung et al. (1999). The nonlinear dynamics is not considered in these (kinematic) controllers, so the complex computation of dynamics can be avoided and the controller design can be simplified considerably. However, these controllers do not always produce high performance, and there is no guarantee of stability at the high speed Shang and Cong (2010). Unlike the kinematic control strategies, full dynamic model of parallel manipulator is taken into account in the dynamic control strategies. So, the nonlinear dynamics of the manipulator can be compensated and higher performance can be achieved with dynamic strategies. Traditional dynamic strategies such as the augmented PD (APD) and the computed-torque controllers were implemented in Cheng et al. (2003),Li and Xu (2004),Paccot et al. (2009). Model-based adaptive controllers have been proposed in Honegger et al. (1997),Honegger et al. (2000),Craig (1988),Sartori-Natal et al. (2009). All mentioned controllers were designed in the joint space. Nevertheless, we are usually concerned about the trajectory tracking in the task space. Especially for the parallel manipulators with redundant actuators, where the effect of the redundant actuators to the end-effector motion can be fully considered Shang and Cong (2010). In the task space, the PID, the augmented PD (APD) and the computed torque controller have been compared in Paccot et al. (2009). In Shang et al. (2009), a nonlinear computed torque controller was designed in order to overcome the problem that its PD algorithm is not robust against modeling errors and nonlinear frictions. For the case of parallel manipulators with redundant actuation, adaptive controllers were designed in the task space to take into account the effect of redundant actuation in Shang and Cong (2010),Wang et al. (2009).

The main objective of the present work was to reach very high accelerations with a simple control approach that would have a small computation time and would be able to maintain the good tracking performance. The idea of this controller consists in using a PID in the Cartesian space to cope with actuation redundancy issues, and to add computed torque inputs based on a simplified but efficient dynamic model. It will be shown that this "computed torque" may become as simple as adding Cartesian and articular accelerations feedforward terms.

This paper is organized as follows. In section 1, a brief description of the R4 parallel manipulator is presented. The proposed control approach is detailed in section 2. Section 3 is devoted to the pick-and-place trajectory generation. The experimental results are presented in section 4. A discussion about the conclusions and future works is made in section 5.

1. R4 PARALLEL MANIPULATOR

1.1 Description of the R4 robot

The R4 parallel manipulator (cf. Fig. 1) has the following main characteristics:

(1) 3-*dof* (translations along x-y-z axis) and 4 actuators (redundantly actuated),
(2) Each motor has a maximum torque of $127N.m$,
(3) A workspace of at least a cylinder of 300 mm radius and 100 mm height.

Its CAD schematic view and its side view are shown in Fig. 1. Its geometrical parameters are summarized in table 1 and illustrated in Fig. 2.

1.2 Simplified Direct Dynamics

Some simplifications on the dynamics of the robot were made during its design phase, in order to evaluate which configuration would be the most optimal in terms of performance and cost:

- Joint frictions were neglected, as the components of the robot were designed in order to have very small frictions between them,
- The inertia of the forearms was also neglected, and their masses were split in two parts each being artificially considered to be located at both ends of the forearms (half of the mass is transferred to the end of the arm whereas the other half is transferred to the traveling plate) as illustrated in Fig. 3,
- Gravity acceleration was not taken into account since the case studies considered very high accelerations.

These assumptions are discussed in Pierrot et al. (2009) and in Nabat (2007).

Table 1. Geometric Parameters

r_b [m]	r_{tp} [m]	l_i [m]	L_i [m]
0.135	0.05	0.2	0.53

The expression of R4's simplified direct dynamic model is given by Corbel et al. (2010):

$$\ddot{x} = (M_{tot} + {J_m}^T I_{tot} J_m)^{-1} J_m (\Gamma - I_{tot} \dot{J}_m \dot{x}) \qquad (1)$$

Table 2. Dynamics Parameters

M_{tp} [kg]	$M_{forearm}$ [kg]	I_{act} [kg.m^2]	I_{arm} [kg.m^2]
0.2	0.065	0.003	0.005

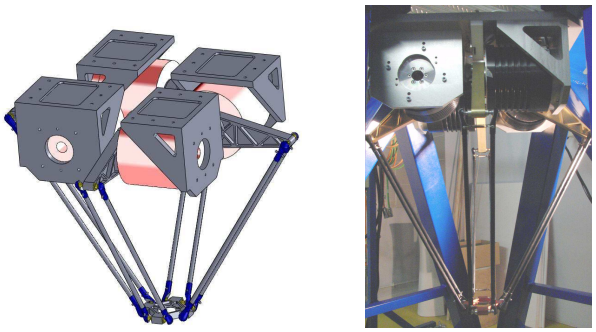

Fig. 1. The R4 parallel manipulator: Schematic view of the CAD design (left), side view of the robot prototype (right)

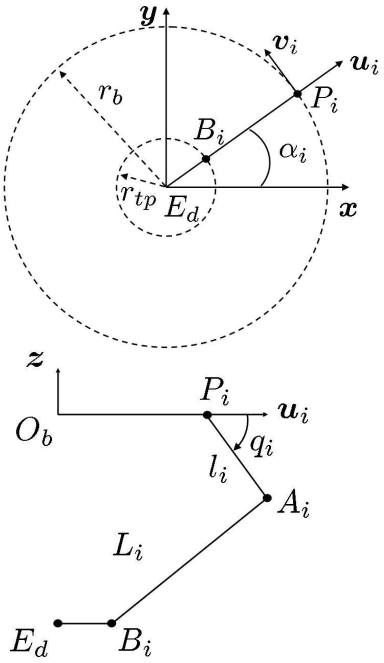

Fig. 2. The R4 parallel manipulator geometric parameters: Top view (top), side view (bottom)

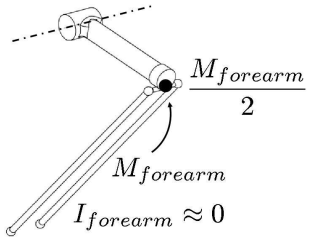

Fig. 3. Forearms mass simplification

where $\dot{x} \in \mathbb{R}^m$ and $\ddot{x} \in \mathbb{R}^m$ are the Cartesian velocities and accelerations; $M_{tot} = M_{tp} + n\frac{M_{forearm}}{2}$ is a diagonal matrix with m diagonal terms, being M_{tp} the mass of the traveling plate, $M_{forearm}$ the mass of the forearm and m the number of degrees-of-freedom (m=3); $I_{tot} = I_{act} + I_{arm} + \frac{{l_i}^2 M_{forearm}}{2}$ is a diagonal matrix with n diagonal

terms, where I_{act} and I_{arm} are the inertia of the actuators and the inertia of the arms, respectively; $J_m \in \mathbb{R}^{n\times m}$ and $\dot{J}_m \in \mathbb{R}^{n\times m}$ are the inverse Jacobian matrix and its first derivative, respectively; and $\Gamma \in \mathbb{R}^n$ represents the torques applied by the motors, being n the number of motors ($n = 4$). For further details on the mechanical design of the R4 parallel manipulator, the reader is referred to Corbel et al. (2010).

1.3 Actuation redundancy and its effects on control

As mentioned in section , the R4 parallel manipulator is redundantly actuated (4 motors and 3 dof). This characteristic has important advantages in terms of mechanical capabilities of the robot, but in terms of control, new issues arise: not only classical articular control schemes are unable to deal with dynamic effects on the Cartesian space, but they are also unable to cope with the actuation redundancy (the integral term will be disturbed by kinematic inconsistencies).

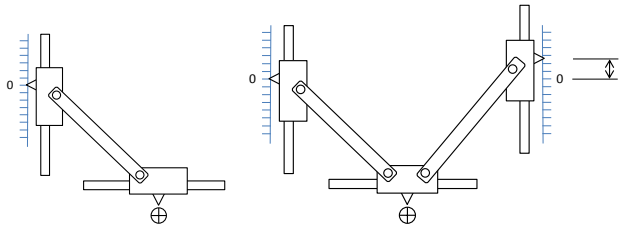

Fig. 4. Illustration of a non-redundant (left) and a redundantly actuated system (right)

This issue is illustrated in Fig. 4. In this figure, the joint space is represented by the linear motors that move vertically and the Cartesian space is represented by the end-effector that moves horizontally. When the system is not redundantly actuated (in this example, it has one measuring scale in joint space and 1 dof in the Cartesian space), it is always possible to converge to a zero joint space error (which has a "0" mark). In the case of a redundantly actuated system (two measuring scales in joint space and 1 dof in the Cartesian space), any geometric error (due to machining inaccuracies, assembly errors, backlash, thermal expansion, etc.) will make it impossible to get all the measuring scales to reach a zero error at the same time. Thus the joint space error vector will never be zero, and this error will always have an effect on the integral term of the controller.

In order to deal with these issues, it is better to implement the control law in Cartesian space; it will be shown in the following that such a controller can easily be completed by a dual-space feedforward that has an effect similar to the computed torque.

2. PROPOSED CONTROL SCHEME: A DUAL-SPACE FEEDFORWARD CONTROLLER

The dual-space feedforward controller consists basically in a PID in the Cartesian space and a feedforward of both desired Cartesian/articular accelerations to improve the tracking performance. This control approach is illustrated in Fig. 5:

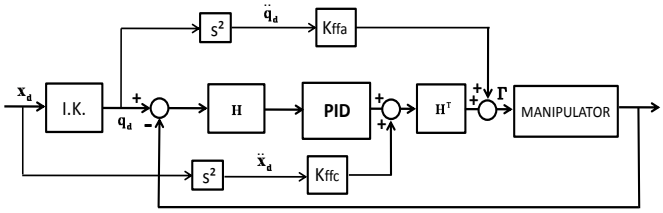

Fig. 5. Block diagram of the proposed dual-space controller

The desired trajectory is given in the Cartesian space (x_d). As only the joint positions are measured (q_m), this desired trajectory is converted to the joint space (q_d) through the inverse kinematics of the robot Corbel et al. (2010), such that the corresponding tracking error can be obtained. The joint tracking errors (Δq) must then be reconverted to the Cartesian space in order to be used by the PID controller. As the joint tracking errors are assumed to be significantly small, and the sampling time (Δt) is of only $0.1ms$ ($10^{-4}s$), let $\frac{\Delta q}{\Delta t} \simeq \frac{dq}{dt}$. Then, it is recalled that:

$$\dot{q} = J_m \dot{x} \tag{2}$$

This relation has an unique solution, but in the case of redundantly actuated systems ($n > m$), the inverse relation will have infinite solutions. In order to cope with this issue, the pseudo-inverse of J_m is used instead (the pseudo-inverse has the property of generating a solution with the minumum Euclidian norm). Therefore, one has:

$$\dot{x} = J_m^+ \dot{q} = H\dot{q} \tag{3}$$

where H is the pseudo-inverse of J_m, that is $H = J_m^+ = ({J_m}^T J_m)^{-1} {J_m}^T$. The following relation between the joint errors and the Cartesian errors (Δx) can then be obtained:

$$\frac{dx}{dt} = H\frac{dq}{dt} \Rightarrow \frac{\Delta x}{\Delta t} \simeq H\frac{\Delta q}{\Delta t} \Rightarrow \Delta x \simeq H\Delta q \tag{4}$$

The resulting forces (f) to be applied on the end-effector will be the sum of the Cartesian PID with the feedforward of the desired Cartesian accelerations (which were obtained by deriving the desired Cartesian trajectories twice). Now, the resulting forces need to be converted to the joint space, as the control inputs that will be sent to the robot are the torques (Γ) to be applied by the motors. For this purpose, it is known that from Eq. 3, the following relation can be obtained:

$$\Gamma = H^T f \tag{5}$$

The desired joint trajectories are also derived twice in order to obtain the desired accelerations for its feedforward term. The following control law is then proposed:

$$\Gamma = H^T f + K_{ffa}\ddot{q}_d \tag{6}$$

being $f = K_p e + K_i \int e(t)dt + K_d \frac{de(t)}{dt} + K_{ffc}\ddot{x}_d$ the force applied on the traveling plate, $e = \Delta x$, K_p, K_i and K_d are the Cartesian PID gains, K_{ffc} the Cartesian acceleration feedforward gain and K_{ffa} is the joint acceleration feedforward gain.

The PID in the Cartesian space was tuned experimentally through the procedure of small steps. The feedforward gains were calculated analytically from the dynamic model of the R4 parallel manipulator as follows.

2.1 Calculation of the feedforward gains

In order to calculate the feedforward gains of the dual-space controller, it is necessary to take into consideration the dynamics of the system, which is represented by Eq. 1, recalled below:

$$\ddot{x} = (M_{tot} + {J_m}^T I_{tot} J_m)^{-1} {J_m}^T (\Gamma - I_{tot} \dot{J}_m \dot{x}) \quad (7)$$

where $M_{tot} = M_{tp} + n\frac{M_{forarm}}{2} = 0.33kg$ and $I_{tot} = I_{act} + I_{arm} + l^2\frac{M_{forearm}}{2} = 0.012kg.m^2$. By multiplying both sides by $(M_{tot} + {J_m}^T I_{tot} J_m)$, one has:

$$(M_{tot} + {J_m}^T I_{tot} J_m)\ddot{x} = {J_m}^T (\Gamma - I_{tot} \dot{J}_m \dot{x}) \quad (8)$$

which results in:

$$M_{tot}\ddot{x} + {J_m}^T I_{tot} J_m \ddot{x} = {J_m}^T \Gamma - {J_m}^T I_{tot} \dot{J}_m \dot{x} \quad (9)$$

The torques (Γ) are separated on the left side, and the following expression is obtained:

$${J_m}^T \Gamma = M_{tot}\ddot{x} + {J_m}^T I_{tot} J_m \ddot{x} + {J_m}^T I_{tot} \dot{J}_m \dot{x} \quad (10)$$

Both sides are then multiplied by the pseudo-inverse of ${J_m}^T$ (which will be named H^T):

$$\Gamma = H^T M_{tot}\ddot{x} + I_{tot} J_m \ddot{x} + I_{tot} \dot{J}_m \dot{x} = H^T M_{tot}\ddot{x} + I_{tot}(J_m \ddot{x} + \dot{J}_m \dot{x}) \quad (11)$$

If one takes into consideration that $(J_m\ddot{x} + \dot{J}_m\dot{x})$ is equal to the articular acceleration vector $(\ddot{q})$, the final expression arises:

$$\Gamma = H^T M_{tot}\ddot{x} + I_{tot}\ddot{q} \quad (12)$$

By direct analysis of Fig. 5, the value of the gains that should multiply $\ddot{x}_d$ and $\ddot{q}_d$ are, respectively, $K_{ffc} = M_{tot} = 0.33$ and $K_{ffa} = I_{tot} = 0.012$. It was shown that, due to the simple dynamic model, the feedforward terms which would compensate for the effects of the dynamics of the system are simply the known parameters M_{tot} and I_{tot}. The gains of the proposed control scheme are presented in table 3.

Table 3. Parameters of the Proposed Controller

K_p	K_i	K_d	K_{ffc}	K_{ffa}
8000	600	40	0.33	0.012

3. TRAJECTORY GENERATION

In this section, two case studies will be presented and detailed. The first one consists in a spiral movement (cf. Fig. 6) that was implemented for a maximum acceleration of 20G (which provided a frequency of 6.5 revolutions per second) on the Cartesian PID and on the proposed dual-space Cartesian/articular controller. The second one consists in a double pick-and-place trajectory (Figs. 7 and 8) that was implemented for a maximum acceleration of 40G only with the dual-space controller (for safety reasons).

3.1 First case study: Spiral movements in X-Y plane

The desired X-Y trajectory is described as follows:

$$\begin{cases} x_d = K_{mod}\ 0.125\ sin(13\pi t) \\ y_d = K_{mod}\ 0.125\ sin(13\pi t + \frac{\pi}{2}) \end{cases} \quad (13)$$

being $K_{mod} = 0.5\ sin(\frac{2\pi t}{15} + \frac{3\pi}{2} - \frac{2\pi}{5})$ a modulation function that guarantees a smooth variation of the circle's radius in order to avoid an abrupt start/finish of experiments. The obtained curve is illustrated in Fig. 6. This experiment has the following procedure:

- The robot goes to its initial position $(0, 0, -0.55)m$ and stops,
- The radius of the circular movement increases smoothly until it reaches $0.125m$ and then decreases smoothly until the robot stops.

The objective of this case study is to evaluate the trajectory tracking performance that would be obtained by the addition of the joint acceleration feedforward to the Cartesian PID controller. As will be detailed in section 4, this performance improvement allowed for a safer increase of the acceleration/velocity of the robot until 40G, which was achieved on the second case study.

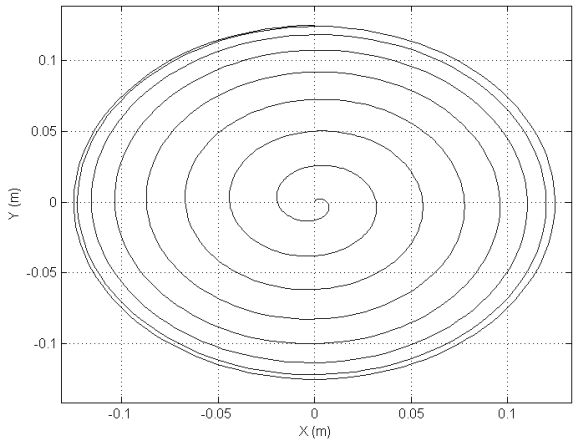

Fig. 6. Top view of the trajectory used in the first case study (spiral in the X-Y plane)

3.2 Second case study: 3D pick-and-place movements

The objective of this case study is to evaluate the capability of the proposed control approach to deal with very high accelerations/velocities in a pick-and-place task. The desired trajectory was chosen such that movements of different distances would have to be performed in the same amount of time, which would require different accelerations/velocities for each one of them, demonstrating the good applicability of the proposed control scheme. The sequence of movements that was executed in this case study is the following:

(1) **Pick 1 - Place 1**: From (-0.1,0.1)m to (0.1,-0.1)m,
(2) **Place 1 - Pick 2**: From (0.1,-0.1)m to (0.1,0.1)m,
(3) **Pick 2 - Place 2**: From (0.1,0.1)m to (-0.1,-0.1)m,
(4) **Place 2 - Pick 1**: From (-0.1,-0.1)m to (-0.1,0.1)m.

Each movement was performed in $0.07s$ ($0.28s$ for the whole cycle) and their maximum height was equal to $5cm$.

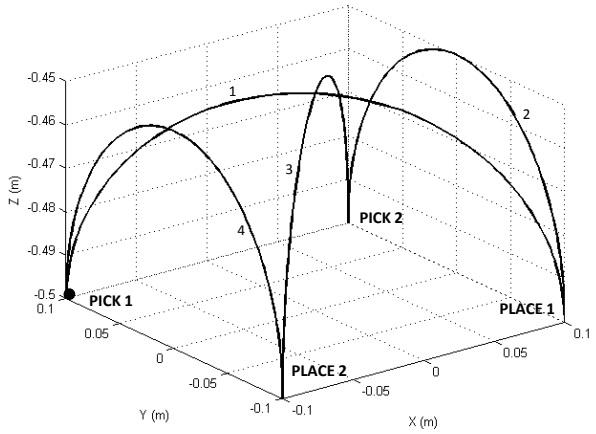

Fig. 7. Isometric view of the trajectory used in the second case study (3D pick-and-place)

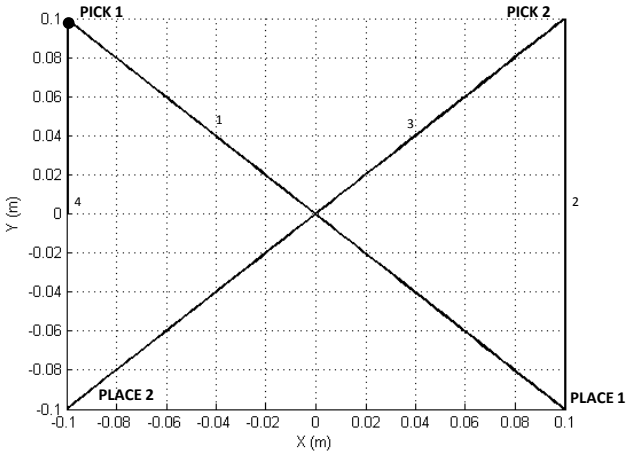

Fig. 8. Top view of the trajectory used in the second case study (3D pick-and-place)

The trajectory generation algorithm used in this case was the polynomial interpolation of degree five presented in Khalil and Dombre (2004). This algorithm guarantees the continuity of the movement in position, velocity and also in acceleration. The idea is to reach a desired final position from a given initial position through the following function:

$$x_f = x_i + r(t)\Delta x, \quad for \;\; 0 \leq t \leq t_f \tag{14}$$

where

$$r(t) = 10(\frac{t}{t_f})^3 - 15(\frac{t}{t_f})^4 + 6(\frac{t}{t_f})^5 \tag{15}$$

being x_i, x_f the initial and final positions, respectively, $r(t)$ the function that represents the trajectory between the two positions (being its limits equal to $r(0) = 0$ and $r(t_f) = 1$), $\Delta x = x_f - x_i$ and t_f the duration of the movement (chosen by the user). An illustrative example of this method is given in Fig. 9 for the X-axis desired trajectory between $[-0.1, 0.1]m$ (together with its first and second time-derivatives), being possible to confirm that this algorithm can provide a continuous signal for position, velocity and also for acceleration.

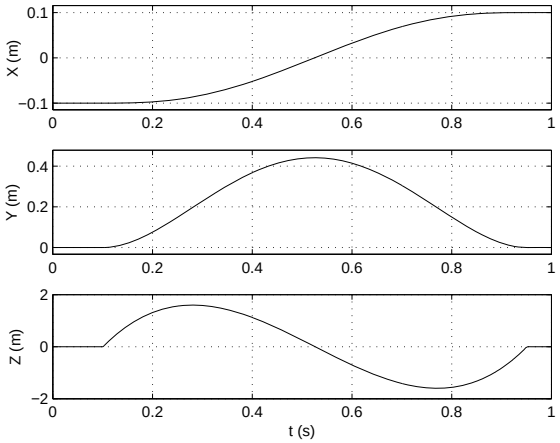

Fig. 9. Example of the trajectory generated by the proposed method

4. REAL-TIME EXPERIMENTAL RESULTS

The objective of this section is to present and discuss the real-time experimental results obtained by the application of the proposed control schemes described in section 2 on the parallel manipulator R4 described in section 1, in order to track the reference trajectories detailed in section 3.

The control schemes were implemented in Simulink/Matlab, being compiled and uploaded to a XPC/Target computer, which managed the real-time task with a sampling frequency of 10KHz, which corresponds to a sampling time of $0.1ms$.

4.1 First case study: Spiral movements in X-Y plane

The obtained results of this scenario are given by figures 10-13. Fig. 10 illustrates the movement along X-axis (similar for Y-axis, with a delay of 90). The robot goes from an arbitrary position to the desired initial position $(0, 0, -0.55)m$ and then the amplitude of the circle starts to increase until it reaches $0.125m$ (reaching a maximum acceleration of 20G), then it decreases in the same way until the robot stops. In order to compare the performance of both controllers, figures 11-13 show a zoom at the time interval of maximum amplitude.

By analyzing Fig. 11, it is possible to notice that the dual-space controller provided a considerably better tracking performance than the classical Cartesian PID. While the former kept the tracking error between $[-4.62, 5.33]mm$ (4% of peak-to-peak error), the latter kept it between

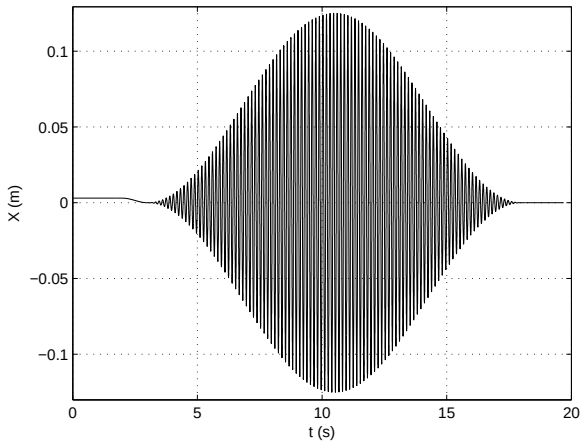

Fig. 10. Demonstration of the trajectory of X-axis

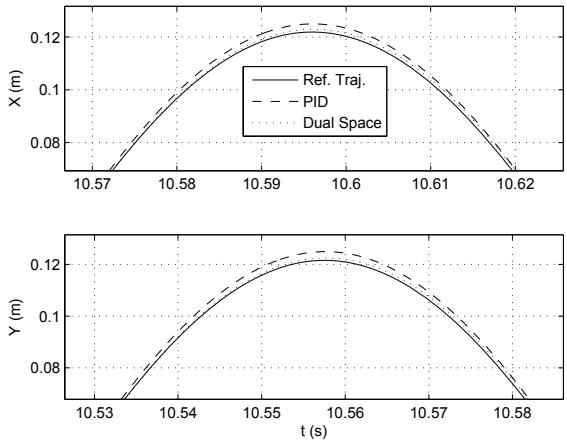

Fig. 11. Zoom on the trajectory tracking for the PID controller (dots) and for the dual-space controller (dashed)

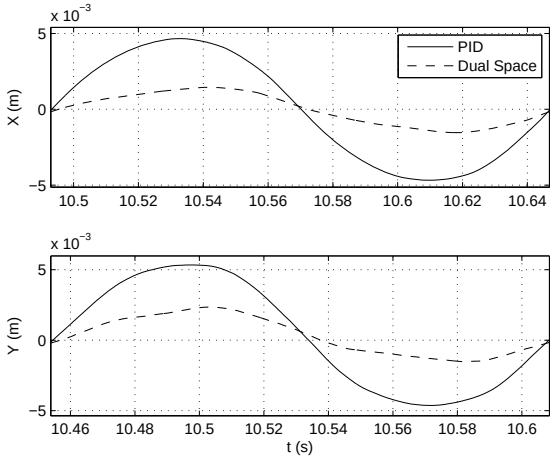

Fig. 12. Tracking errors for the PID controller (solid) and for the dual-space controller (dashed)

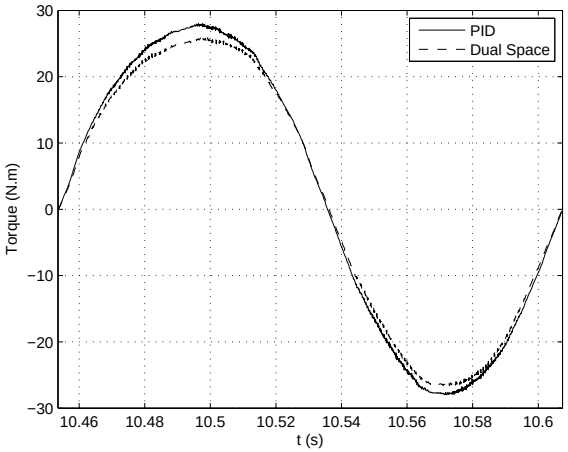

Fig. 13. Torques for the PID controller (solid) and for the dual-space controller (dashed)

$[-1.55, 2.34]mm$ (1.56%) (cf. Fig. 12), which means a peak-to-peak improvement of approximately 60%. The Root Mean Square Error (RMSE) shows an equivalent improvement in performance ($1.3mm$ against $3.6mm$, which means an improvement of approximately 64%). Another advantage of the dual-space controller was that its control signal had an approximately 6% smaller peak-to-peak ($[-26.4, 26.2]Nm$ against $[-28, 28]Nm$) than the Cartesian PID (cf. Fig. 13). These results are summarized in table 4.

With the conclusion that the dual-space controller can provide a considerably better tracking performance than the Cartesian PID, the latter was discarded for the next case study.

Table 4. Performance comparison between the proposed control approach and the Cartesian PID controller

Performance	**PID**	**Dual-space**
Error peaks	$[-4.62, 5.33]mm$ (4%)	$[-1.55, 2.34]mm$ (1.56%)
RMSE	$3.6mm$	$1.3mm$
Control signals	6% smaller peak-to-peak value	

4.2 Second case study: 3D pick-and-place movements

In the following experiment, the robot goes from an arbitrary position to the desired initial position $(-0.1, 0.1, -0.55)m$ and then two cycles of the proposed pick-and-place trajectory start, as shown in Fig. 14. This experiment has been also registered on the accompanying video. The obtained results for this scenario are depicted in figures 14-18.

By analyzing Fig. 15, it is possible to notice that the proposed control scheme was able to maintain a good tracking performance even for such fast movements. Fig. 16 shows that the dual-space controller kept the tracking errors of the X-Y axis between $[-3.21, 4.4]mm$ (3.8% of peak-to-peak error) and the tracking errors of the Z-axis between $[-6.66, 6.27]mm$ (25.9% of peak-to-peak error). Even though the errors in the Z-axis may seem relatively big, it is important to emphasize that its peak errors happen during the displacement of the platform, while it is known that the control objective of a pick-and-place task is

to obtain the best precision around the stop points (which take place on the periodical bottom of the Z-axis reference trajectory, being the circled neighbourhood of $t = 4.25s$ an example). In Figs. 15 and 16 it is clear that around the stop points the errors are satisfactorily small (smaller than $1.5mm$). The generated torques illustrated in Fig. 17 show that none of the motors has approached its limit of $127Nm$. The results are summarized in table 5.

Table 5. Tracking performance obtained with the proposed controller for the 40G pick-and-place trajectory

Performance	**Dual-space**
Error peaks (X-Y)	$[-3.21, 4.4]mm$ (3.8%)
Error peaks (Z) / displacement	$[-6.66, 6.27]mm$ (25.9%)
Error peaks (Z) / stop points	$[-1.5, 1.5]mm$ (1.5%)
Control Signals	Smooth and far from motor limits

In Fig. 18, the measured Cartesian acceleration is presented, and shows that the obtained acceleration was slightly higher than 40G ($\frac{400.3}{9.81} m/s^2 \rightarrow 40.8G$). This measurement was made with an external accelerometer (Silicon Designs 2460-200, which senses accelerations in all 3 axis and has a measurement limit of $\pm$ 200G) attached to the end-effector. Its model is presented in Fig. 19*. It is important to emphasize that the data acquisition of the accelerometer was made with a different equipment, which was not activated exactly at the same time as the robot. So its displayed time is slightly different from the time displayed in Figs. 15-17.

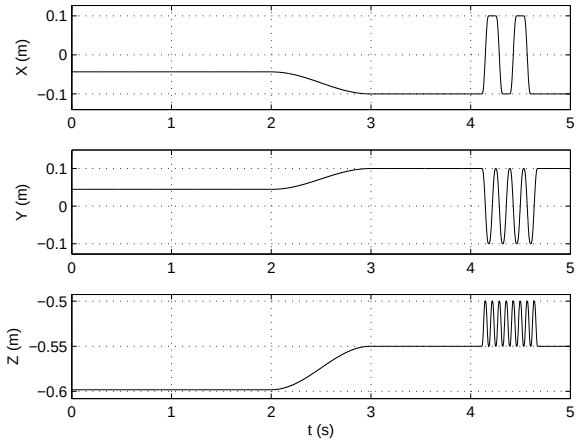

Fig. 14. Illustration of the experiment (including initialization)

5. CONCLUSIONS AND FUTURE WORKS

This paper dealt with the control of the redundantly actuated parallel manipulator R4 for very fast pick-and-place applications. The proposed control scheme consisted in a PID in the Cartesian space complied with a feedforward of the desired acceleration in both Cartesian and articular spaces, firstly for a spiral movement in X and Y-axis (maximum acceleration of 20G) and then for a pick-and-place task (maximum acceleration of 40G). By analyzing the results of the first case study, it was possible to notice

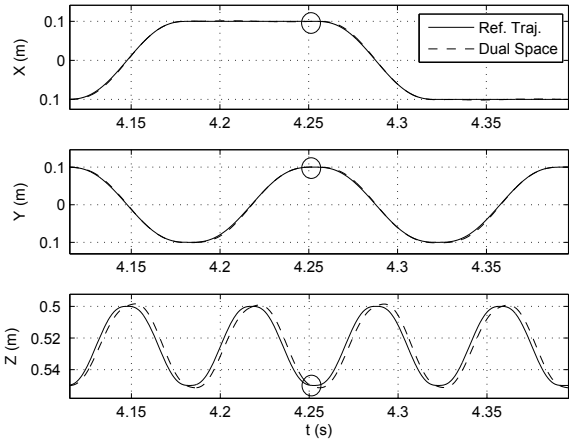

Fig. 15. Trajectory tracking for 40G

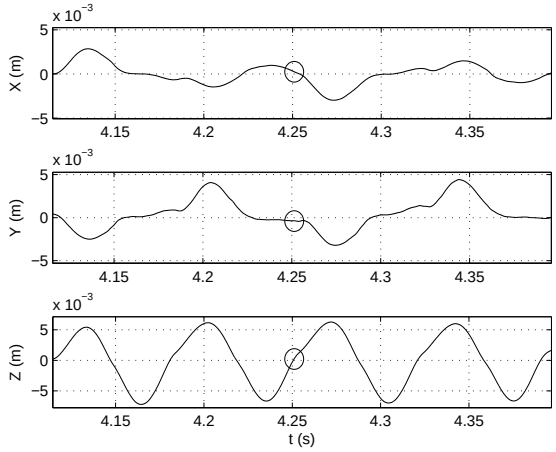

Fig. 16. Tracking errors for 40G

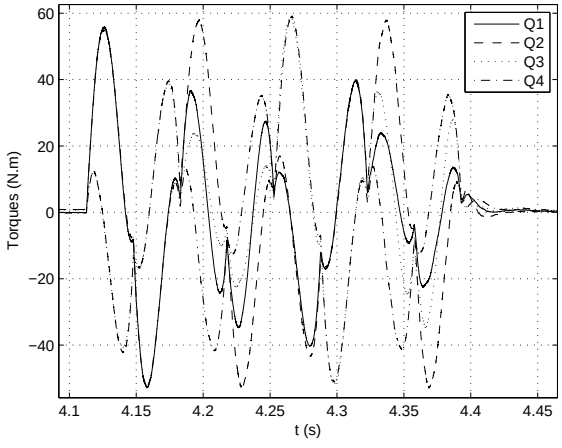

Fig. 17. Evolution of torques vs. time generated by the proposed controller

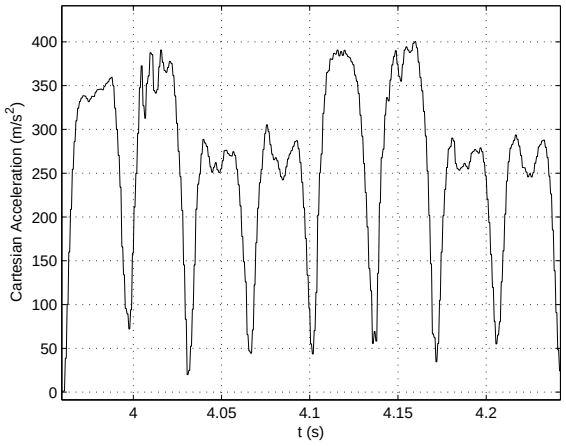

Fig. 18. Measurement of the Cartesian acceleration through an external accelerometer

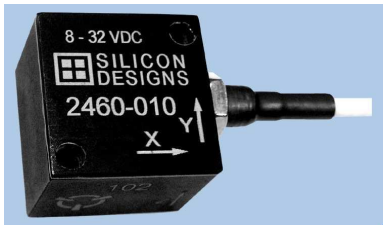

Fig. 19. External accelerometer used in the experiments*

that the proposed controller had a considerably better performance than only the Cartesian PID controller, being the latter discarded for the second case study for safety reasons. It was then possible to notice that the proposed dual-space Cartesian/articular controller was able to provide a good tracking performance even in such fast pick-and-place tasks (equivalent to more than 425 pick-and-place cycles per minute). In the future, other control approaches to be investigated/proposed will be evaluated for higher accelerations and/or for different load conditions.

REFERENCES

Begon, P., Pierrot, F., and Dauchez, P. (1995). Robot control and parameter estimation with only joint position measurements. *Proc. IEEE Int. Conf. Robot. Autom.*, 1178–1183.

Cheng, H., Yiu, Y.K., and Li, Z.X. (2003). Dynamics and control of redundantly actuated parallel manipulators. *IEEE Trans. Mechatronics*, 8(4), 483–491.

Chung, I.F., Chang, H.H., and Lin, C.T. (1999). Fuzzy control of a six-degree motion platform with stability analysis. *Proc. IEEE Int. Conf. Syst. Man. Cybern.*, 325–330.

Clavel, R. (1988). Delta, a fast robot with parallel geometry. *International Symposium on Industrial Robots*, 91–100.

Corbel, D., Gouttefarde, M., Company, O., and Pierrot, F. (2010). Towards 100g with pkm. is actuation redundancy a good solution for pick-and-place? 4675–4682.

Craig, J.J. (1988). *Adaptive Control of Mechanical Manipulators*. Addison-Wesley Publishing Company.

Ghorbel, F.H., Chatelat, O., Gunawardana, R., and Longchamp, R. (2000). Modeling and set point control of closed-chain mechanisms: theory and experiment. *IEEE Trans. Control Syst. Technol*, 8(5), 801–815.

Honegger, M., Brega, R., and Schweitzer, G. (2000). Application of a nonlinear adaptive controller to a 6 dof parallel manipulator. *Proc. IEEE Conf. Robotics Automat.*, 2, 1930–1935.

Honegger, M., Codourey, A., and Burdet, E. (1997). Adaptive control of the hexaglide, a 6 dof parallel manipulator. In *In IEEE International Conference on Robotics and Automation*.

Khalil, W. and Dombre, E. (2004). *Modeling, identification & control of robots*. Butterworth-Heinemann.

Kock, S. and Schumacher, W. (1998). A parallel x-y manipulator with actuation redundancy for high-speed and active-stiffness applications. *Proc. IEEE Conf. Robotics Automat.*, 2295–2300.

Li, Q. and Xu, F.X. (2004). Control performance improvement of a parallel robot via the design for control approach. *Mechatronics*, 14(8), 947–964.

Nabat, V. (2007). Robots parallles nacelle articule - du concept la solution industrielle pour le pick-and-place. *PhD. dissertation, Universit Montpellier II, Montpellier, France*.

Ouyang, P.R., Zhang, W.J., and Wu, F.X. (2002). Nonlinear pd control for trajectory tracking with consideration of the design for control methodology. *Proc. IEEE Int. Conf. Robot. Autom.*, 41264131.

Paccot, F., Andreff, N., and Martinet, P. (2009). A review on the dynamic control of parallel kinematic machines: Theory and experiments. *Int. J. Rob. Research*, 28(3), 395–416.

Park, F.C. and Kim, J.W. (1999). Singularity analysis of closed loop kinematic chains. *ASME Trans. J. Mech. Des.*, 121(1), 32–38.

Pierrot, F., Baradat, C., Nabat, V., Company, O., Krut, S., and Gouttefarde, M. (2009). Above 40g acceleration for pick-and-place with a new 2-dof pkm. *Proc. of the IEEE International Conference on Robotics and Automation*, 1794–1800.

Roberts, R.G., Yu, H.G., and Maciejewski, A.A. (2008). Fundamental limitations on designing optimally fault-tolerant redundant manipulator. *IEEE Trans. Robotics*, 24(5), 1224–1237.

Sartori-Natal, G., Chemori, A., Pierrot, F., and Company, O. (2009). Nonlinear dual mode adaptive control of par2: a 2-dof planar parallel manipulator, with real-time experiments. *Proc. IEEE/RSJ Int. Conf. Intel. Robotics Systems.*, 2114–2119.

Shang, W.W. and Cong, S. (2010). Nonlinear adaptive task space control for a 2-dof redundantly actuated parallel manipulator. *Nonlinear Dynamics*, 59(1).

Shang, W.W., Cong, S., Li, Z.X., and Jiang, S.L. (2009). Augmented nonlinear pd controller for a redundantly actuated parallel manipulator. *Advanced Robotics*, 2(12).

Su, Y.X., Duan, B.Y., Zheng, C.H., Zhang, Y.F., Chen, G.D., and Mi, J.W. (2004). Disturbance-rejection high-precision motion control of a stewart platform. *IEEE Trans. Control Syst. Technol.*, 12(3), 364–374.

Wang, L., Lu, Z.T., Liu, X.P., Liu, K.F., and Zhang, D. (2009). Adaptive control of a parallel robot via backstepping technique. *Int. J. Systems, Contr. and*

Comm., 1(3), 312–324.

Wu, F.X., Zhang, W.J., Li, Q., and Ouyang, P.R. (2002). Integrated design and pd control of high-speed closed-loop mechanisms. *J. Dyn. Syst. Meas. Control*, 124(4), 522–528.

Yang, T., Ma, J., and et al., Z.G.H. (2006). Parameter identification and tuning of the servo system of a 3-hss parallel kinematic machine. *International Journal of Advanced Manufacturing Technology*, 31(5).

Yi, Y., Mcinroy, J.E., and Chen, Y.X. (2006). Fault tolerance of parallel manipulators using task space and kinematic redundancy. *IEEE Trans. Robotics*, 22(5), 1017–1021.

Zhiyong, Y. and Huang, T. (2004). A new method for tuning pid parameters of a 3-dof reconfigurable parallel kinematic machine. *Proc. IEEE Conf. Robotics Automat.*, 2249–2254.